



**HAL**  
open science

## Biostable highly aligned polyurethane fibres for the potential application of small calibre vascular grafting

Chin Joo Tan, Ang Bee Chin, Andri Andriyana, Grégory Chagnon

### ► To cite this version:

Chin Joo Tan, Ang Bee Chin, Andri Andriyana, Grégory Chagnon. Biostable highly aligned polyurethane fibres for the potential application of small calibre vascular grafting. *Materials Science and Engineering Technology / Materialwissenschaft und Werkstofftechnik*, 2020, 51 (11), pp.1473-1480. 10.1002/mawe.202000053 . hal-03850125

**HAL Id: hal-03850125**

**<https://hal.science/hal-03850125>**

Submitted on 12 Nov 2022

**HAL** is a multi-disciplinary open access archive for the deposit and dissemination of scientific research documents, whether they are published or not. The documents may come from teaching and research institutions in France or abroad, or from public or private research centers.

L'archive ouverte pluridisciplinaire **HAL**, est destinée au dépôt et à la diffusion de documents scientifiques de niveau recherche, publiés ou non, émanant des établissements d'enseignement et de recherche français ou étrangers, des laboratoires publics ou privés.

**Article type:** Article

**Title:** Biostable highly aligned polyurethane fibres for the potential application of small calibre vascular grafting

**Authors:** C. J. Tan<sup>1, 2, 3</sup>, B. C. Ang<sup>1, 4, \*</sup>, A. Andriyana<sup>1, 2</sup>, G. Chagnon<sup>5</sup>

<sup>1</sup>University of Malaya, Faculty of Engineering, Centre of Advanced Materials, 50603, KUALA LUMPUR, MALAYSIA

<sup>2</sup>University of Malaya, Faculty of Engineering, Department of Mechanical Engineering, 50603, KUALA LUMPUR, MALAYSIA

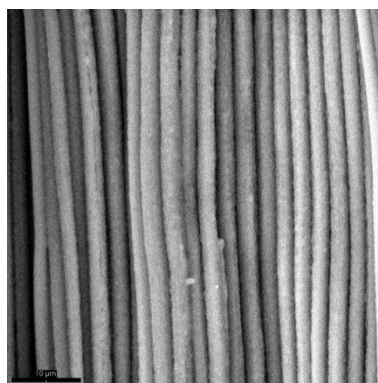
<sup>3</sup>IOP Specialists Sdn. Bhd., Klang Central Industrial Park, 41400, KLANG, MALAYSIA

<sup>4</sup>University of Malaya, Faculty of Engineering, Department of Chemical Engineering, 50603, KUALA LUMPUR, MALAYSIA

<sup>5</sup>Université Grenoble Alpes, CNRS, CHU Grenoble Alpes, Grenoble INP, TIMC-IMAG, F-38000, GRENOBLE, FRANCE

\*Corresponding author: E-mail: amelynang@um.edu.my

**Graphical Abstract:**



In this study, highly aligned polyurethane fibres are fabricated through a facile dry spinning technique in the view to assess its biostability for the potential application of small calibre vascular grafting. The biostability of the fibres is evaluated in terms of physical, mechanical and chemical properties. Results show that the fibres do not show any obvious deterioration in all the three properties mentioned even after 24 weeks of immersion in simulated body fluid.

**Abstract:** Synthetic vascular grafting is necessary when the autografting is not possible in some cases. Conventional polyethylene terephthalate and expanded polytetrafluoroethylene vascular grafts are found to be effective for diameter bigger than 6 mm but not for the diameter smaller than 4 mm due to the compliance mismatch and thrombogenicity. Endothelization on the surface of the graft can reduce the risks of compliance mismatch and thrombogenicity. In order to catalyze the endothelization process, fibrous morphology similar to the extracellular matrix of our body is preferable in the vascular grafts. Apart from that, the biostability of the grafts is also an essential element to be considered as the biodegradation may reduce the efficiency of the grafts. Many polyurethanes have been recognised as biostable materials. Hence, in this study, highly aligned polyurethane fibres are fabricated using a facile dry spinning technique in the view of providing effective sites for endothelization process to occur. These fibres are immersed into the simulated body fluid for as long as 24 weeks before conducting the biostability characterisations. The biostability is assessed in three aspects, physical, mechanical and chemical properties. Results show that the fibres do not have observable or significant deteriorations in all the three aspects mentioned.

**Keywords:** Polyurethane / fibres / biostable / vascular / grafts

## 1 Introduction

Vascular grafting has been an effective remedy to vascular diseases for decades. Autografting by using the veins or arteries in the patient's body with high patency rate for years is common in United States where 400000 operations are conducted yearly [1].

In some cases, autografting is not possible due to the unavailability of suitable arteries or veins [2]. This is when the synthetic vascular grafts come in handy. At the early stage, inert materials with the least interaction with the blood and tissues are the choices for these synthetic vascular grafts. Polyethylene terephthalate (PET) and expanded polytetrafluoroethylene (ePTFE) are the most common materials in vascular grafting with good performance for decades. However, the good performances of the PET and ePTFE are only limited to large vascular grafts with diameter more than 6 mm. It is found that the both materials mentioned are not suitable for small vascular grafts with diameter less than 4 mm [3, 4]. As a result, researches are conducted to sought for more appropriate small diameter synthetic vascular grafts.

The most commonly encountered problems in vascular grafting are compliance mismatch and thrombogenicity. The compliance mismatch can lead to intimal hyperplasia which ends up narrowing the lumen and thus affecting the flow of blood. In order to overcome these problems, homogenous functional endothelization on the vascular grafts can be an effective solution [5]. Thus, the initial design philosophy of synthetic vascular graft by using inert materials is deemed to be unrealistic. This is because the vascular grafts need to allow the attachment of endothelial cells for endothelization to occur.

Another crucial criterion for a competent synthetic vascular graft is the biostability [6]. The biological environment in the body may trigger the biodegradation

of the graft causing deterioration in physical, mechanical and chemical properties [7]. In addition, the degraded by products may be harmful to the patient. Hence, the synthetic vascular grafts must be able to resist biodegradation in the body.

In the literature, many polyurethanes have been recognised as biostable materials<sup>8</sup>. However, these biostability studies are conducted on non-fibrous polyurethane samples [6, 8, 9]. The biostability studies on polyurethane fibrous samples are relatively less [10]. Despite being the same polyurethane, non-fibrous and fibrous samples may have different properties as the same polyurethane with different microstructures or morphology can have different properties or behaviours [11-13]. Hence, it is vital to study the biostability of the polyurethane fibrous samples. In the application wise, the study on the biostability of polyurethane fibrous samples is also important due to the fact that the fibrous morphology is similar to extracellular matrix of the body which can contribute to the endothelization process [14, 15]. Hu et al. [16] conducted in vitro study with randomly aligned polyurethane fibrous sample for the vascular grafting application. Homogenous endothelization is observed on the grafts with patency rate more than 80% for 24 weeks, much higher than the PTFE graft which is only 33% for the same duration. Thus, in this study, the same polyurethane is used to fabricate the fibrous sample for biostability test. However, the polyurethane fibres in this study are highly aligned as highly aligned fibres are found to be more effective in the endothelization process [17-19].

## **2 Methodology**

### **2.1 Materials**

MDI-polyester/polyether polyurethane in pellet form (CAS number: 68084-39-9) is the raw material used to fabricate the highly aligned polyurethane fibres. N,N-Dimethylformamide (DMF) and Tetrahydrofuran (THF) with purity more than 99% are the solvents used to dissolve the polyurethane pellets. These solvents and the polyurethane pellets are bought from Sigma Aldrich and used as received without further processing.

The simulated body fluid (SBF) is prepared by dissolving Hank's balanced salt (without sodium bicarbonate and phenol red, Sigma Aldrich) and sodium bicarbonate (reagent grade) in distilled water [20].

### **2.2 Fabrication of highly aligned polyurethane fibres**

A 15 wt% polyurethane solution is prepared by dissolving the polyurethane pellets into a mixture of DMF and THF solvents in the ratio of 1:1. Then, a syringe with needle of 27 gauge size is filled with the solution. Finally, the fibres fabrication is conducted by a simple dry spinning setup [21, 22], *Figure 1*. The solution injection rate is set at 0.05 ml/hr. Initially, a solution jet is manually drawn from the syringe to the rotating collector in a distance of 15 cm. After that, the fibres wind on the rotating collector with a speed of approximately 100 rpm.

### **2.3 Biostability test of highly aligned polyurethane fibres**

For the biostability test, the fibres are immersed into the SBF. The durations of immersion are 2, 4, 8, 12 and 24 weeks respectively. All these simulated body fluids with samples immersed inside are kept at body temperature, 37 °C using a water bath.

#### *2.3.1 Mass change measurement*

The initial masses of the samples denoted by  $M_i$  are measured, whereas the masses of the samples after immersion in SBF,  $M_f$  are measured before and after removing all the absorbed water by drying in oven at 40 °C for every immersion duration. Then, the percentages change in mass,  $M_{\%}$  are calculated based on this equation,  $M_{\%} =$

$$\frac{M_f - M_i}{M_i} \times 100\%.$$

#### *2.3.2 pH measurement*

The pH values of the SBF are measured after every immersion duration using a pH meter.

#### *2.3.3 Surface characterisation*

The surface characterisations of the dried fibres after every immersion duration are conducted using Phenom ProX desktop scanning electron microscope (SEM). The average diameters of the fibres after every immersion duration are measured.

#### *2.3.4 Uniaxial mechanical tensile test*

Monotonic tensile mechanical tests under the strain rate of 0.001 s<sup>-1</sup> are conducted on the dried samples after every immersion duration in the SBF using the Shimadzu AGS-X Series Universal Tensile Testing Machine.

### 2.3.5 Fourier Transform Infrared Spectroscopy (FTIR)

FTIR is used to detect the chemical interactions between the fibres and SBF. Both the fibres and SBF before and after every immersion duration are characterised using Nicolet iS10 FTIR spectrometer from Thermo Scientific. The spectra range from 400 to 4000 wavenumber with a resolution of 4  $\text{cm}^{-1}$ .

## 3 Results and discussion

### 3.1 Physical characterisations

The micrographs of the fabricated polyurethane fibres are taken using SEM, *Figure 2*. These fibres are highly aligned in the vertical direction of the micrograph which corresponds to the circumferential direction of the rotating collector.

The most obvious change in the polyurethane fibrous samples after immersing in the SBF is the swollen effect. The increment in the mass after removing from the SBF bathes of the fibrous samples is within the range of 100% to 140% regardless of the immersion durations, *Figure 3*. As a result, these SBF rich fibrous samples can be favourable sites for the body cells attachment for endothelization purpose.

In the view of physical degradation, the amount of mass lost is deemed to be the easiest and the most direct indication in most studies [23-26]. Normally, the lost in mass is accompanied with the loss of molecular weight, crystallinity and mechanical strength. The mass loss of the polyurethane fibrous sample in this study is measured after all the moistures are removed from the sample by drying. It appears that the mass loss in the polyurethane fibrous samples is negligible, less than 1% regardless of the SBF immersion durations, *Figure 4a* which agrees with the average diameters of the

fibres that do not change significantly in the range of 2.66 to 3.24  $\mu\text{m}$ , Figure 4b. This negligible mass lost may suggest that no degradation has occurred. Nevertheless, further tests are needed to verify this suggestion. In this study, the mechanical properties of the polyurethane fibrous samples are evaluated for validation which will be further discussed in the next section.

### **3.2 Mechanical characterisations**

Effects of the moisture on the mechanical properties of polyurethane is noteworthy in the literature [27-29]. The glass transition temperature is found to be lowered with moisture trapped inside the microstructure of the polyurethane, which in turn changes the mechanical properties and behaviours of the polyurethane. Despite of that, the effects of moisture are not permanent. The glass transition temperature will return to the initial value after the moistures are removed totally.

As discussed in the previous paragraph, the effects of moisture on the mechanical properties of the polyurethane are temporarily which is not in the interest of this study. Instead, the permanent damage to the polyurethane fibrous samples due to the hydrolytic degradation in SBF [25] is of the interest in this study. Hence, the fibrous samples are dried totally before the mechanical tests and validated using FTIR spectra, *Figure 7*. The peaks of hydroxyl groups in water molecules are not found in the spectra of all the dried fibres.

The initial moduli and ultimate tensile strengths of the polyurethane fibrous samples in the direction of the fibres alignment after different SBF immersion durations are plotted, *Figure 5*. The initial moduli of the polyurethane fibrous samples range from 7.63 to 8.00 MPa, whereas the ultimate tensile strengths range from 6.54 to 6.98 MPa. These ultimate tensile strengths are similar to the longitudinal ultimate tensile strength

of Saphenous vein with the average value of 5.38 MPa [30]. Both the initial moduli and ultimate tensile strengths are having insignificant changes after different SBF immersion durations in agreement with the insignificant mass lost in the fibrous samples as shown in Figure 4a. It is clear now that there is no observable degradation in terms of mass lost and mechanical properties at the macroscopic level.

### **3.3 Chemical characterisations**

#### *3.3.1 Simulated body fluid*

The pH values of the SBF is measured after every immersion duration. As a control, the pH values of a SBF sample without polyurethane fibrous samples immersed in it is also measured. The results are plotted, *Figure 6*. It is observed that both the SBF with or without the fibrous samples immersed in them are having similar pH values after every immersion duration. The pH values fluctuate between pH 6 to 7 which are almost neutral. This can be another indication that the polyurethane fibres do not undergo hydrolytic degradation as the process will release acidic groups into the SBF due to the breakage of ester or urethane bonds causing the pH values to drop [31, 32].

Further analysis on SBF after the immersion at different durations is conducted by using FTIR, *Figure 7*. There are 3 distinctive peaks can be observed in the spectra at the wavenumbers, 602 / 604, 1635 and 3335 / 3337  $\text{cm}^{-1}$ . These peaks are corresponding to the hydroxyl bonds in the water molecules [33] which consists of more than 90% of the content in the SBF. No additional peak is observed in the spectra after every immersion duration which may suggest that no degraded products from the polyurethane fibres are found in the SBF.

### 3.3.2 Highly aligned polyurethane fibres

Polyurethane with solvents trapped inside the microstructure is found to have lower modulus [34]. This external factor may influence the initial moduli measured and go against the objective to study the mechanical properties of the polyurethane fibres due to hydrolytic degradation solely. In order to prevent the incomplete drying of the solvent, THF with much higher volatility are mixed with DMF [35, 36] to spin the fibres in this study. The absence of the residual solvents in the polyurethane fibres is verified by FTIR, *Figure 8*. It can be suggested that there is no residual solvent in the polyurethane fibres as the FTIR spectra of the polyurethane pellet and fibres match each other perfectly without any extra peak that may exist due to the residual DMF or THF solvent.

In the literature, the degradation of the polyurethane is due to breakage of the urethane linkages which correspond to the C=O and NH functional groups. The wavenumbers corresponding to some characteristic peaks of the bonds in polyurethanes are tabulated, *Table 1*. Due to the breakage of the urethane linkages, the intensity of the transmittance peaks corresponds to the C=O and NH groups will become lower than the undegraded polyurethane [37, 38]. The FTIR spectra of the dried polyurethane fibres match each other in terms of intensities and peaks regardless of the immersion durations, *Figure 8*. This may mean that the chemical structure of the polyurethane fibres remains intact even after 24 weeks of immersion in the SBF bath.

## 4 Conclusion

In this study, highly aligned polyurethane fibres are fabricated through a simple dry spinning technique. The alignment of the fibres is verified by SEM. Biostability tests are conducted on the fibres due to the potential of the fibres in the application of vascular grafting. The fibres are immersed in SBF for different durations of 2, 4, 8, 12

and 24 weeks. Then, the biostability of the fibres after immersing in SBF is evaluated from three aspects, physical, mechanical and chemical properties. Physical characterisations show that the mass change and the average diameter change of the fibres are negligible. In term of mechanical properties, the initial modulus and ultimate tensile strength of the fibres are having insignificant changes as well. Lastly, the chemical structures of the fibres also remain intact after immersing in SBF. As a conclusion, the fibres fabricated in this study are biostable even after 24 weeks of immersion in SBF.

### **Acknowledgement**

The authors greatly appreciate the financial support from University of Malaya (PG109-2016A, RP041A-17AET and IIRG012A-2019) and from Embassy of France in Malaysia.

### **5 References**

- [1] D.S. Baim, *J. Am. Coll. Cardiol.*, **2003**, *42*, 1370.
- [2] M. Desai, A.M. Seifalian, G. Hamilton, *Eur. J. Cardio-Thorac. Surg*, **2011**, *40*, 394.
- [3] L. Xue, H.P. Greisler, *J. Vasc. Surg.*, **2003**, *37*, 472.
- [4] R.Y. Kannan, H.J. Salacinski, P.E. Butler, G. Hamilton, A.M. Seifalian, *J. Biomed. Mater. Res. Part B*, **2005**, *74B*, 570.
- [5] P.F. Sánchez, E.M. Brey, J.C. Briceño, *J. Tissue Eng. Regen. Med.*, **2018**, *12*, 2164.
- [6] S. Kim, S. Liu, *ACS Biomater. Sci. Eng.*, **2018**, *4*, 1479.
- [7] H.J. Salacinski, M. Odlyha, G. Hamilton, A.M. Seifalian, *Biomaterials*, **2002**, *23*, 2231.

- [8] D. Cozzens, U. Ojha, P. Kulkarni, R. Faust, S. Desai, *J. Biomed. Mater. Res. Part A*, **2010**, 95A, 774.
- [9] L. Rueda, B. Fernandez d'Arlas, M.A. Corcuera, A. Eceiza, *Polym. Degrad. Stabil.*, **2014**, 108, 195.
- [10] D. Cozzens, X. Wei, R. Faust, *J. Polym. Sci. Pt. B-Polym. Phys.*, **2013**, 51, 452.
- [11] A. Pedicini, R.J. Farris, *Polym.*, **2003**, 44, 6857.
- [12] T. Sunada, M. Kuriyagawa, T. Kawamura, K.-h. Nitta, *e-Journal of Soft Materials*, **2011**, 7, 8.
- [13] U. Stirna, B. Lazdiņa, D. Vilsone, M.J. Lopez, M.d.C. Vargas-Garcia, F. Suárez-Estrella, J. Moreno, *J. Cell. Plast.*, **2012**, 48, 476.
- [14] J.H. Oh, J.S. Lee, K.M. Park, H.T. Moon, K.D. Park, *Macromol. Res.*, **2012**, 20, 1150.
- [15] F. Ahmed, N.R. Choudhury, N.K. Dutta, A. Zannettino, R. Knott, *Biomacromolecules*, **2013**, 14, 3850.
- [16] Z.-j. Hu, Z.-l. Li, L.-y. Hu, W. He, R.-m. Liu, Y.-s. Qin, S.-m. Wang, *BMC Cardiovasc. Disord.*, **2012**, 12, 115.
- [17] C.Y. Xu, R. Inai, M. Kotaki, S. Ramakrishna, *Biomaterials*, **2004**, 25, 877.
- [18] W. He, Z. Hu, A. Xu, R. Liu, H. Yin, J. Wang, S. Wang, *Cell Biochem. Biophys.*, **2013**, 66, 855.

- [19] C.S. Wong, X. Liu, Z. Xu, T. Lin, X. Wang, *J. Mater. Sci. Mater. Med*, **2013**, *24*, 1865.
- [20] N.I. Zainal Abidin, A.D. Atrens, D. Martin, A. Atrens, *Corrosion Sci.*, **2011**, *53*, 3542.
- [21] C.J. Tan, A. Andriyana, B.C. Ang, G. Chagnon, *Mater. Res. Express*, **2018**, *5*, 125301.
- [22] C.J. Tan, J.J.L. Lee, B.C. Ang, A. Andriyana, G. Chagnon, M.S. Sukiman, *J. App. Polym. Sci.*, **2019**, *0*, 47706.
- [23] Z. Zhou, Q. Yi, L. Liu, X. Liu, Q. Liu, *J. Macromol. Sci. Part B*, **2009**, *48*, 309.
- [24] M. Żenkiewicz, A. Richert, R. Malinowski, K. Moraczewski, *Polym. Test*, **2013**, *32*, 209.
- [25] J. Brzeska, A. Heimowska, H. Janeczek, M. Kowalczyk, M. Rutkowska, *J. Polym. Environ.*, **2014**, *22*, 176.
- [26] Q. Breche, G. Chagnon, G. Machado, E. Girard, B. Nottelet, X. Garric, D. Favier, *J. Mech. Behav. Biomed. Mater.*, **2016**, *60*, 288.
- [27] B. Yang, W.M. Huang, C. Li, C.M. Lee, L. Li, *Smart Mater. Struct.*, **2003**, *13*, 191.
- [28] W.M. Huang, B. Yang, L. An, C. Li, Y.S. Chan, *Appl. Phys. Lett.*, **2005**, *86*, 114105.
- [29] B. Yang, W.M. Huang, C. Li, L. Li, *Polym.*, **2006**, *47*, 1348.
- [30] B.A. Hamedani, M. Navidbakhsh, H.A. Tafti, *Biomed Eng Online*, **2012**, *11*, 59.
- [31] Z. Wang, L. Yu, M. Ding, H. Tan, J. Li, Q. Fu, *Polym. Chem.*, **2011**, *2*, 601.

- [32] C. Ruan, Y. Hu, L. Jiang, Q. Cai, H. Pan, H. Wang, *J. App. Polym. Sci.*, **2014**, *131*, 19.
- [33] I. Litvak, Y. Anker, H. Cohen, *RSC Adv.*, **2018**, *8*, 28472.
- [34] S. Monaghan, R.A. Pethrick, *Ind. Eng. Chem. Res.*, **2012**, *51*, 11038.
- [35] J. Shawon, C. Sung, *J. Mater. Sci.*, **2004**, *39*, 4605.
- [36] R. Erdem, İ. Usta, M. Akalin, O. Atak, M. Yuksek, A. Pars, *Appl. Surf. Sci.*, **2015**, *334*, 227.
- [37] Y.-L. Luo, Y. Miao, F. Xu, *Macromol. Res.*, **2011**, *19*, 1233.
- [38] S. Sahoo, H. Kalita, S. Mohanty, S.K. Nayak, *J. Polym. Environ.*, **2018**, *26*, 1528.
- [39] A. Asefnejad, M.T. Khorasani, A. Behnamghader, B. Farsadzadeh, S. Bonakdar, *Int. J. Nanomed.*, **2011**, *6*, 2375.
- [40] S. Bonakdar, S.H. Emami, M.A. Shokrgozar, A. Farhadi, S.A.H. Ahmadi, A. Amanzadeh, *Mater. Sci. Eng. C*, **2010**, *30*, 636.
- [41] Y. Kurimoto, M. Takeda, A. Koizumi, S. Yamauchi, S. Doi, Y. Tamura, *Bioresour. Technol.*, **2000**, *74*, 151.

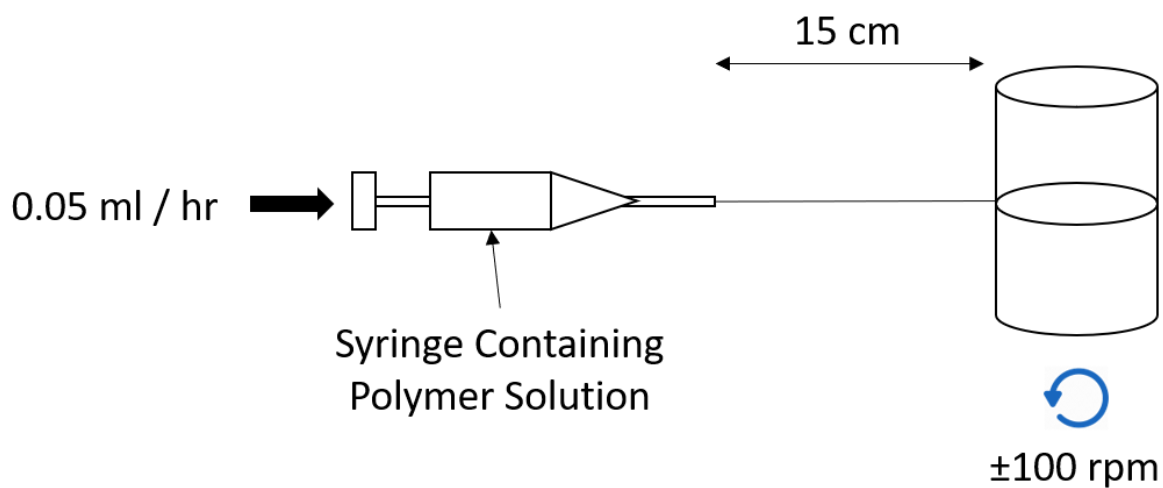


**Figure 1.** Dry spinning setup based on the studies conducted by Tan et al. [21, 22].

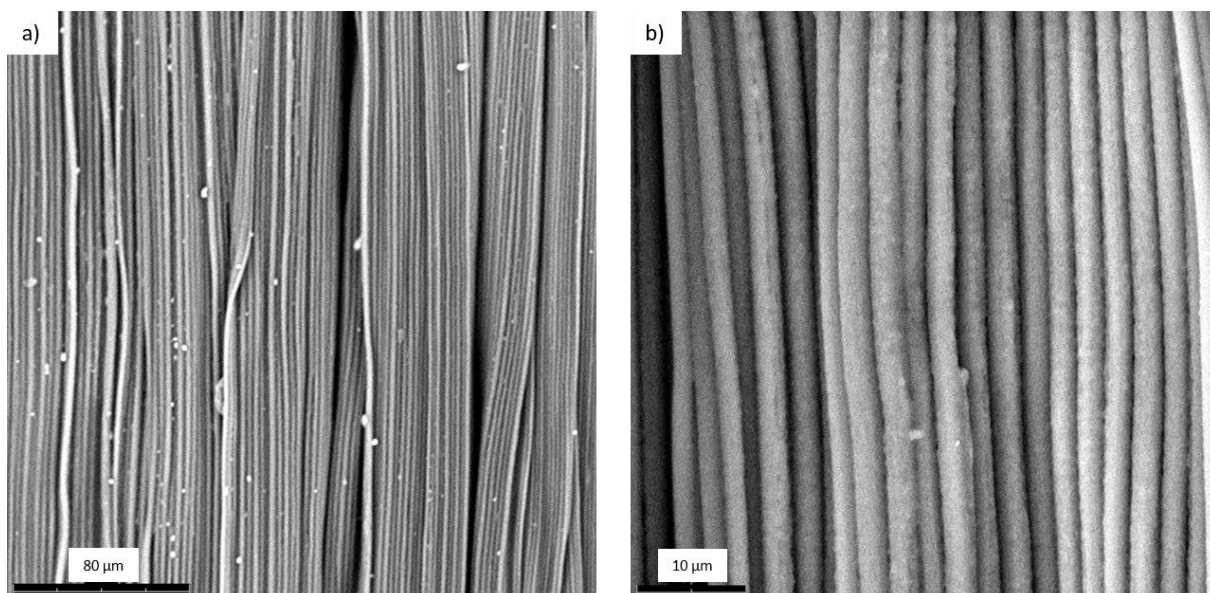


**Figure 2.** SEM micrographs of highly aligned polyurethane fibres under the magnification of (a) 1000 x and (b) 5000 x.

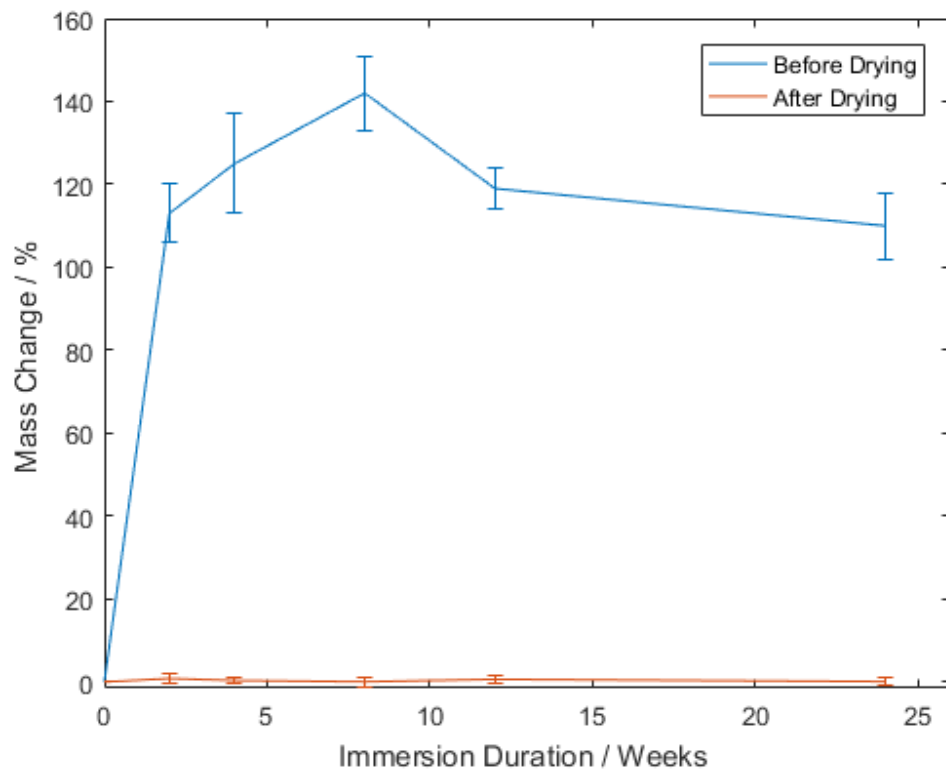


**Figure 3.** Mass change of the highly aligned polyurethane fibres.

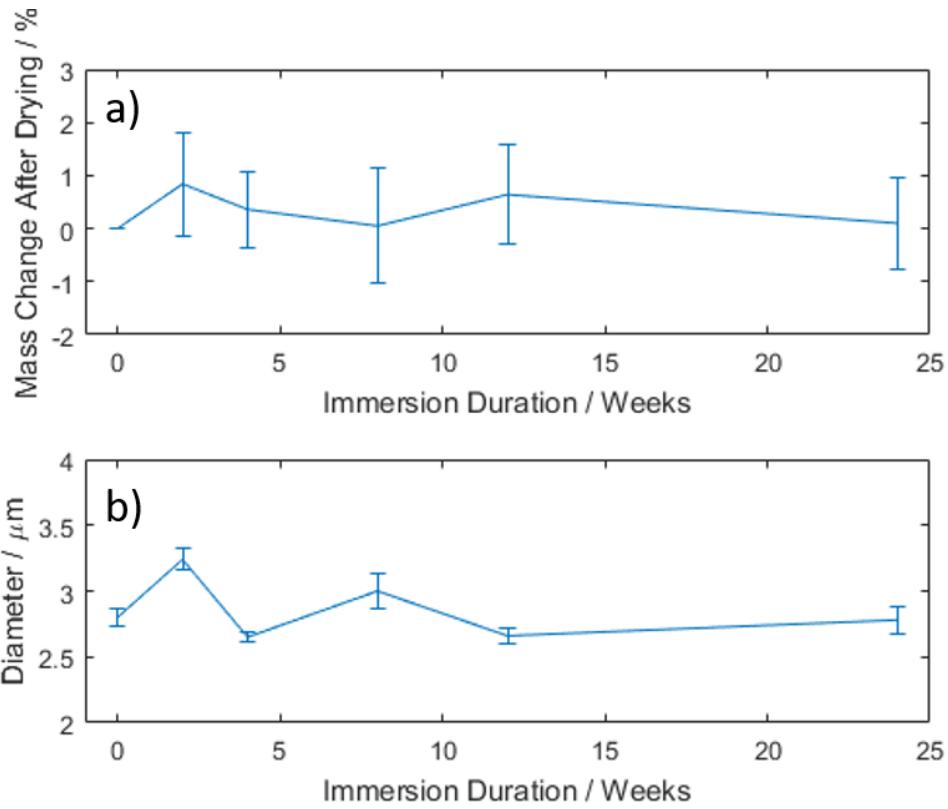


**Figure 4.** (a) Mass change of the highly aligned polyurethane fibres after drying and (b) average diameter of the fibres at different SBF immersion durations.

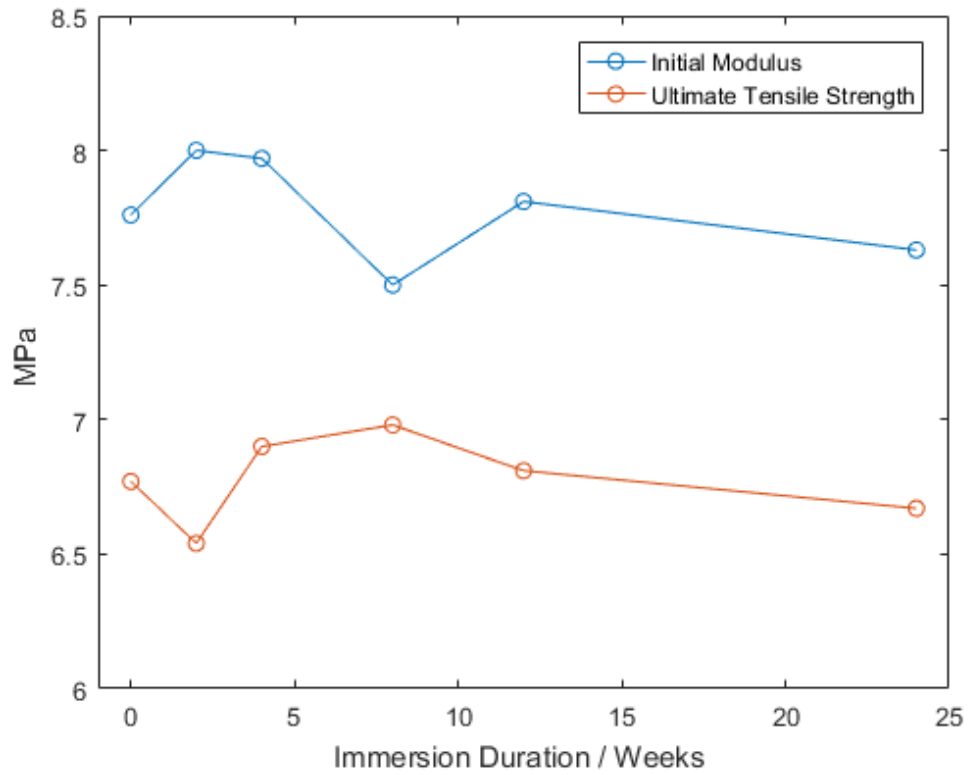


**Figure 5.** Evolution of initial modulus and ultimate tensile strength of the highly aligned polyurethane fibres with the increment in SBF immersion durations.

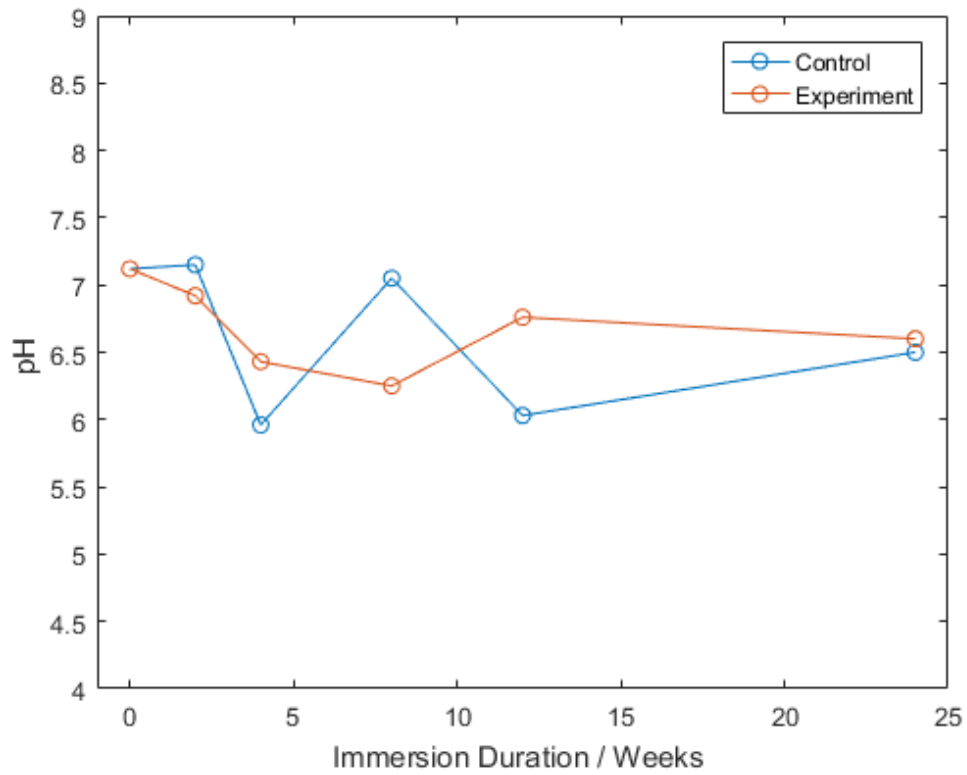


**Figure 6.** pH of the SBF after different immersion durations.

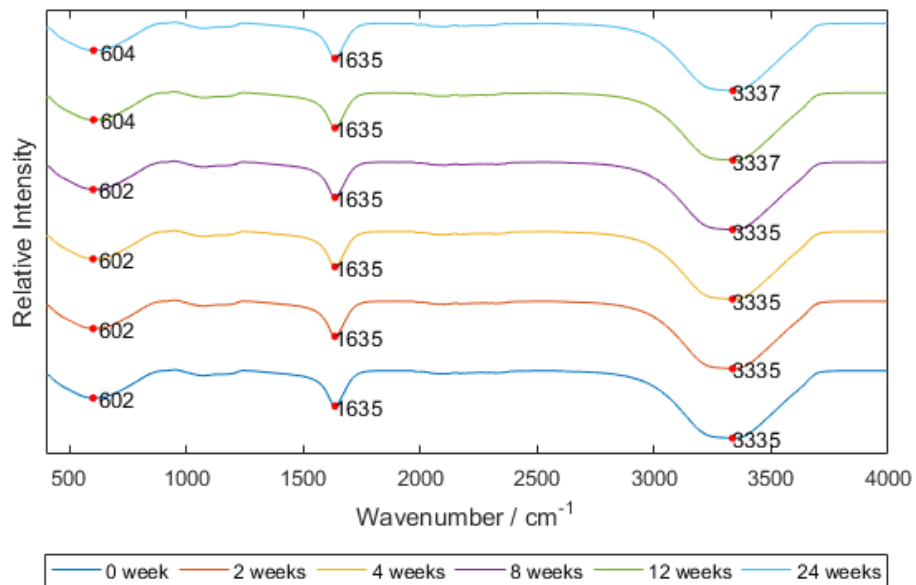


**Figure 7.** FTIR spectra of SBF after different immersion durations.

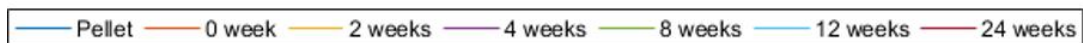
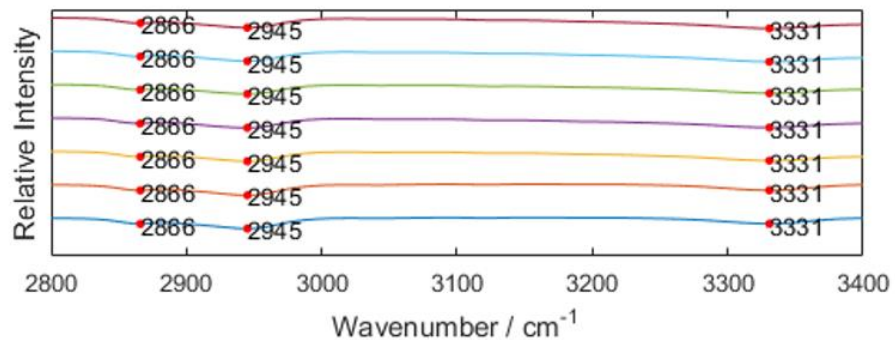
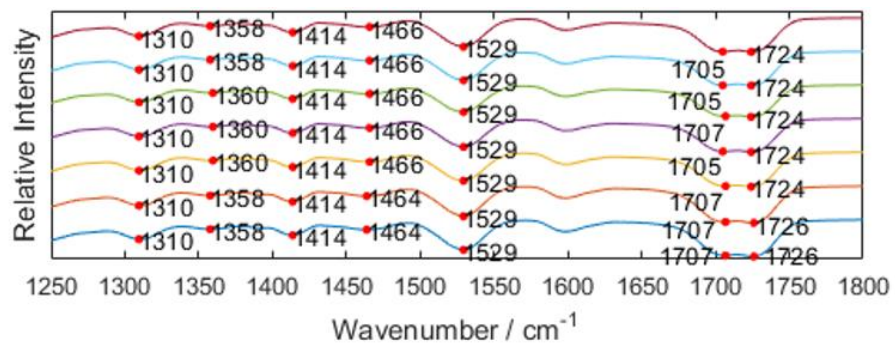


**Figure 8.** FTIR spectra of a polyurethane pellet and the highly aligned polyurethane fibres after different immersion durations.

**Table 1.** Bonds corresponding to the FTIR spectra wavenumbers of the polyurethane [39-41].

<b>Wavenumber / cm<sup>-1</sup></b>	<b>Bond</b>
1310	
1358 / 1360	-CH <sub>2</sub>
1414	
1466 / 1464	
1529	NH
1705 / 1707	H-bond between NH and C=O
1724 / 1726	C=O
2866	-CH <sub>2</sub>
2945	
3331	NH